

PFB-Diff: Progressive Feature Blending Diffusion for Text-driven Image Editing

Wenjing Huang Shikui Tu Lei Xu
Shanghai Jiao Tong University

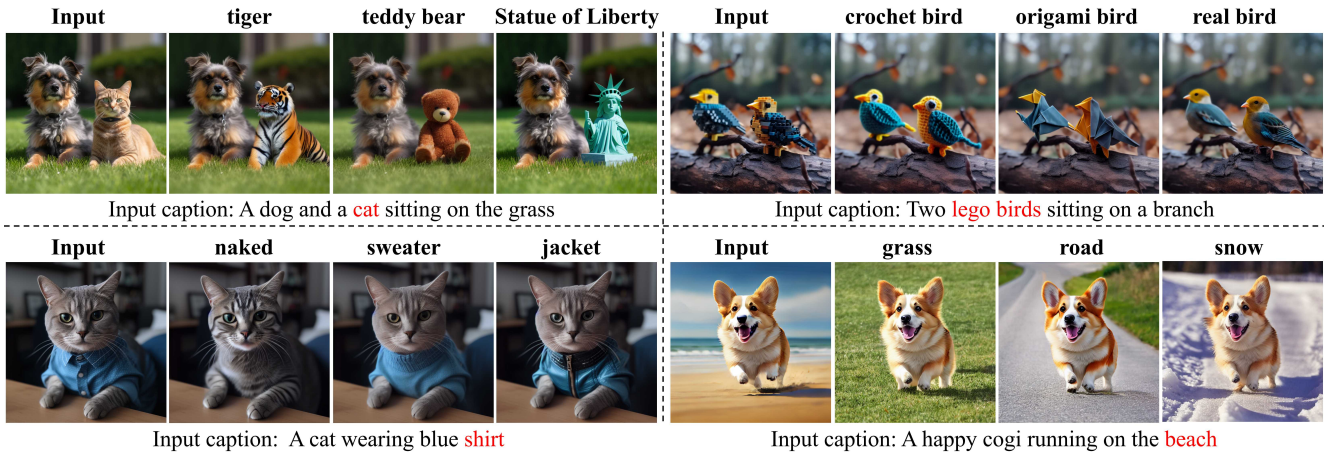


Figure 1. PFB-Diff for real image editing. Given an image, a text query, and a mask that annotates the regions of interest, our method enables text-driven image editing while preserving the irrelevant regions. Our approach can be applied to various tasks, such as object replacement (top-left), secondary object editing (bottom-left), object attribute editing (top-right), and background replacement (bottom-right).

Abstract

Diffusion models have showcased their remarkable capability to synthesize diverse and high-quality images, sparking interest in their application for real image editing. However, existing diffusion-based approaches for local image editing often suffer from undesired artifacts due to the pixel-level blending of the noised target images and diffusion latent variables, which lack the necessary semantics for maintaining image consistency. To address these issues, we propose PFB-Diff, a Progressive Feature Blending method for Diffusion-based image editing. Unlike previous methods, PFB-Diff seamlessly integrates text-guided generated content into the target image through multi-level feature blending. The rich semantics encoded in deep features and the progressive blending scheme from high to low levels ensure semantic coherence and high quality in edited images. Additionally, we introduce an attention masking mechanism in the cross-attention layers to confine the impact of specific words to desired regions, further improving the performance of background editing. PFB-Diff can effectively address various editing tasks, including object/background replacement and object attribute editing.

Our method demonstrates its superior performance in terms of image fidelity, editing accuracy, efficiency, and faithfulness to the original image, without the need for fine-tuning or training.

1. Introduction

Diffusion Models (DM) have garnered significant attention by enabling high-quality and diverse synthesis of images from a given text prompt [10, 17]. Recently introduced large-scale training of diffusion models, such as DALL-E2 [31], Imagen [35], GLIDE [29], and Stable Diffusion [32], have further improved the quality and demonstrated unprecedented semantic generation. Large-scale text-to-image models are trained on enormous amounts of image-caption pairs, resulting in a high capacity for both textual semantic understanding and image synthesis. Given a corresponding text description, they can generate realistic images that match the text description. Such success inspires subsequent efforts to leverage large-scale pre-trained diffusion models for real image editing.

However, extending pre-trained text-to-image frame-

works for personalized editing (e.g. manipulating a specific object in an image) remains a challenging task due to the limited ability to describe desired objects through text. In fact, even the most detailed textual description of an object may yield instances with different appearances. Besides, the editing process should meet the requirements of high accuracy (or image-text alignment), image consistency, irrelevance preservation, and image fidelity. Image consistency measures whether newly generated content in a target region exhibits contextual coherence both semantically and textually. For instance, when adding a teddy bear to a tree branch, it should align with the environment, such as adopting a tree climbing pose (semantic consistency), and seamlessly blend with the original image (texture consistency).

To achieve personalized editing, some pioneering works [12, 21, 34] proposed to learn a unique word to represent the given object and fine-tune pre-trained text-to-image diffusion models on several images containing the same object. By inserting its unique word in various text contexts, they can synthesize the object in diverse scenes and manipulate the object with text guidance. These methods can typically generate high-fidelity images, but sometimes they drastically alter the content of the original image. Besides, these methods cannot fully leverage the generalization ability of the pre-trained model due to the over-fitting issues [44] or language drift problem [34], i.e., the model slowly forgets how to generate subjects of the same class as the target object after fine-tuning. Moreover, the above methods introduce a per-image optimization process, which cannot satisfy the requirement of high efficiency in practical applications.

In contrast, the optimization-free methods [4, 5, 9, 27] perform image editing based on a frozen pre-trained diffusion model and require no optimization or fine-tuning. To seamlessly fuse newly generated content with the original image, they generally apply the diffusion process first on the input image and then conduct the denoising procedure conditioned on both the input image and the text guidance. Throughout the denoising procedure, previous methods spatially blend noised versions of the input image with the text-guided diffusion latent variables at each time step, using either a user-provided mask [4, 5, 27] or a self-predicted mask [9]. Without any fine-tuning or optimization process, the above methods can avoid the language drift problem [34] and run in real time. Additionally, employing the original image and mask for iterative refinement can aid in preserving visual details.

However, the above methods often rely on editing intermediate noisy images [4, 5, 9, 27], which lacks the necessary semantics to preserve the image consistency, resulting in degraded results. Moreover, the newly generated content is not always guaranteed to appear appropriately within predefined regions especially when the given mask conflicts

with the text description (e.g., attempting to generate a rabbit within a giraffe-shaped region), leading to both image-text misalignment and poor image quality.

In this paper, we propose PFB-Diff, a framework adapting pre-trained text-to-image models for text-driven image editing. As an optimization-free method, our method inherits its advantages of efficiency and the ability to fully utilize the pre-trained model’s generalization capabilities. Meanwhile, we propose several novel techniques to overcome the existing issues in previous optimization-free methods, such as image inconsistency and image-text misalignment. We summarize them as follows.

- *Progressive feature blending.* Instead of editing intermediate noisy images, we propose to edit their deep feature maps in the prediction network. Deep features contain rich semantics and thus feature-level editing can ensure semantic and texture consistency in the edited images. The editing is progressively performed from high to low feature levels via multi-scale masks. This approach helps to seamlessly integrate the newly generated content into the original image, resulting in more natural and coherent synthesis results.
- *Masking the word’s attention map.* To restrict the influence of specific words in predefined regions, we propose to mask their attention maps. For example, when editing an image from “a dog sitting on a beach” to “a dog sitting on the snow,” we mask the background area in the attention map of the word “dog.” This ensures that the “dog” does not affect the background area, thereby preserving the original image’s overall layout and avoiding the generation of another dog in the background.

With the above techniques, our approach can simultaneously meet the requirements of image fidelity, image-text alignment, and faithfulness to the original image. As shown in Figure 1, our approach can effectively tackle various editing tasks, such as object/background replacement, secondary object editing, and changing object properties.

2. Related works

Semantic image editing Semantic image editing has received great attention from the vision and graphics community due to its various potential applications. The literature on the use of GANs [14] for image synthesis and editing has exploded since the seminal work by Goodfellow et al. [14]. In recent years, style-based generator [19, 20] emerged as a powerful image synthesis model, and a plethora of recent works [1, 2, 18, 37, 42, 45] tend to explore the rich interpretable semantics inside the latent space of fixed GAN models. For example, Shen et al. [37] and Yang et al. [43] utilize classifiers to analyze StyleGAN [19] and show that a

linear manipulation in \mathcal{W} -space can control a specific target attribute. GANSpace [18] carries out Principal Component Analysis (PCA) in the latent space of generative networks and explores interpretable controls in an unsupervised manner. To archive text-driven image editing, some researchers [3, 6, 13, 19, 30] leverage pre-trained GAN generators [20] and text encoders [30] to progressively optimize the image according to the text prompt. Despite their promising results, GAN-based approaches are typically limited to images from a restricted domain, on which the GAN was trained. This paper targets building a framework that works for generic real-world natural images.

DDPM for semantic editing In the past few years, diffusion models have advanced to achieve state-of-the-art performance regarding quality and mode coverage since the introduction of denoising diffusion probabilistic models [17]. Large-scale diffusion models, such as Imagen [35], DALL-E2 [31], and Stable Diffusion [32], have greatly enhanced the ability to generate images from plain text, known as text-to-image synthesis. Naturally, recent works [4, 5, 9, 21, 27, 34] have attempted to adapt text-guided diffusion models to real image editing, aiming to exploit their rich and diverse semantic knowledge. A slew of studies [12, 21, 22, 34] propose learning a unique word for a given object and fine-tuning the diffusion models case-specifically for different text prompts. These methods usually introduce a case-specific optimization process, which may limit their applications in real time. Another line of research focuses on designing optimization-free methods [4, 5, 8, 9, 26, 27], which require no fine-tuning or optimization and can be easily extended to any pre-trained diffusion models. These methods usually apply the diffusion process first on the input image and then conduct the denoising procedure conditioned on both the input image and text guidance. To preserve details of original images, they often spatially blend noised versions of the input image with the text-guided diffusion latent variables at each time step, using either a user-provided mask [4, 5, 27] or self-predicted one [9]. Notably, Prompt-to-Prompt [15] controls the editing of synthesized images by manipulating the cross-attention maps; however, its editing ability is limited when applied to real images. When combined with Null-text inversion [28], an accurate inversion technique and thus facilitate an intuitive text-based modification of the image, Prompt-to-Prompt [15] can be extended to real image editing. This paper focuses on developing an optimization-free method for image editing, which can be applied to any pre-trained diffusion models and completes image editing within approximately 10 seconds.

3. Preliminaries

Diffusion models. Denoising diffusion probabilistic models (DDPMs) [17] is a class of generative models. Given a set of real data $\mathbf{x}_0 \sim q(\mathbf{x}_0)$, diffusion models aim to approximate the data distribution $q(\mathbf{x}_0)$ and sample from it. The idea is to gradually inject noise into data, and then reverse this process to generate data from noise. The forward noise-injection process is formalized as a Markov chain with Gaussian transitions:

$$q(\mathbf{x}_{1:T}|\mathbf{x}_0) = q(\mathbf{x}_0) \prod_{t=1}^T q(\mathbf{x}_t|\mathbf{x}_{t-1}), \quad (1)$$

$$q(\mathbf{x}_t|\mathbf{x}_{t-1}) = \mathcal{N}\left(\mathbf{x}_t; \sqrt{1 - \beta_t}\mathbf{x}_{t-1}, \beta_t\mathbf{I}\right),$$

where $\beta_t \in (0, 1)$ represent the noise schedule at time t . When T is large enough, the last latent \mathbf{x}_T is nearly an isotropic Gaussian distribution. The reverse denoising process aims to recreate the true sample from a Gaussian noise input, $\mathbf{x}_T \sim \mathcal{N}(\mathbf{0}, \mathbf{I})$, by sampling from $q(\mathbf{x}_{t-1}|\mathbf{x}_t)$ sequentially. Note that if β_t is small enough, $q(\mathbf{x}_{t-1}|\mathbf{x}_t)$ will also be Gaussian. Unfortunately, it is difficult to estimate $q(\mathbf{x}_{t-1}|\mathbf{x}_t)$ as it depends on the unknown data distribution $q(\mathbf{x}_0)$. Instead, a deep neural network p_θ is trained to predict the mean and the covariance of \mathbf{x}_{t-1} given \mathbf{x}_t as input, \mathbf{x}_{t-1} is then sampled from the normal distribution defined by these predicted parameters,

$$p_\theta(\mathbf{x}_{t-1}|\mathbf{x}_t) = \mathcal{N}(\mathbf{x}_{t-1}; \boldsymbol{\mu}_\theta(\mathbf{x}_t, t), \boldsymbol{\Sigma}_\theta(\mathbf{x}_t, t)). \quad (2)$$

Instead of directly estimating $\boldsymbol{\mu}_\theta(\mathbf{x}_t, t)$, Ho et al. [17] suggest predicting the noise $\epsilon_\theta(\mathbf{x}_t, t)$ that was introduced to \mathbf{x}_0 to produce \mathbf{x}_t , following the objective:

$$\min_{\theta} E_{\mathbf{x}_0, \epsilon \sim \mathcal{N}(\mathbf{0}, \mathbf{I}), t \sim \text{Uniform}(1, T)} \|\epsilon - \epsilon_\theta(\mathbf{x}_t, t)\|_2^2. \quad (3)$$

Subsequently, $\boldsymbol{\mu}_\theta(\mathbf{x}_t)$ can be derived using Bayes' theorem,

$$\boldsymbol{\mu}_\theta(\mathbf{x}_t, t) = \frac{1}{\sqrt{\alpha_t}} \left(\mathbf{x}_t - \frac{\beta_t}{\sqrt{1 - \bar{\alpha}_t}} \epsilon_\theta(\mathbf{x}_t, t) \right), \quad (4)$$

where $\alpha_t = 1 - \beta_t$ and $\bar{\alpha}_t = \prod_{i=1}^t \alpha_i$. At the inference time, we start from a random noise $\mathbf{x}_T \sim \mathcal{N}(\mathbf{0}, \mathbf{I})$ and then iteratively apply Eq. (2) to obtain \mathbf{x}_{t-1} from \mathbf{x}_t until $t = 0$. For more details of DDPMs, please refer to [17, 38, 40].

DDIM sampling. Text-guided diffusion models aim to map a random noise vector \mathbf{x}_T and textual condition \mathcal{C} to an output image \mathbf{x}_0 aligned with the given text prompt. Since we aim to accurately reconstruct a given real image, we employ the deterministic DDIM [39] sampling to sequentially remove the noise:

$$\mathbf{x}_{t-1} = \sqrt{\frac{\alpha_{t-1}}{\alpha_t}} \mathbf{x}_t + \left(\sqrt{\frac{1}{\alpha_{t-1}} - 1} - \sqrt{\frac{1}{\alpha_t} - 1} \right) \epsilon_\theta(\mathbf{x}_t, t, \mathcal{C}). \quad (5)$$

Step 1: Forward noise-injection using DDIM encoding

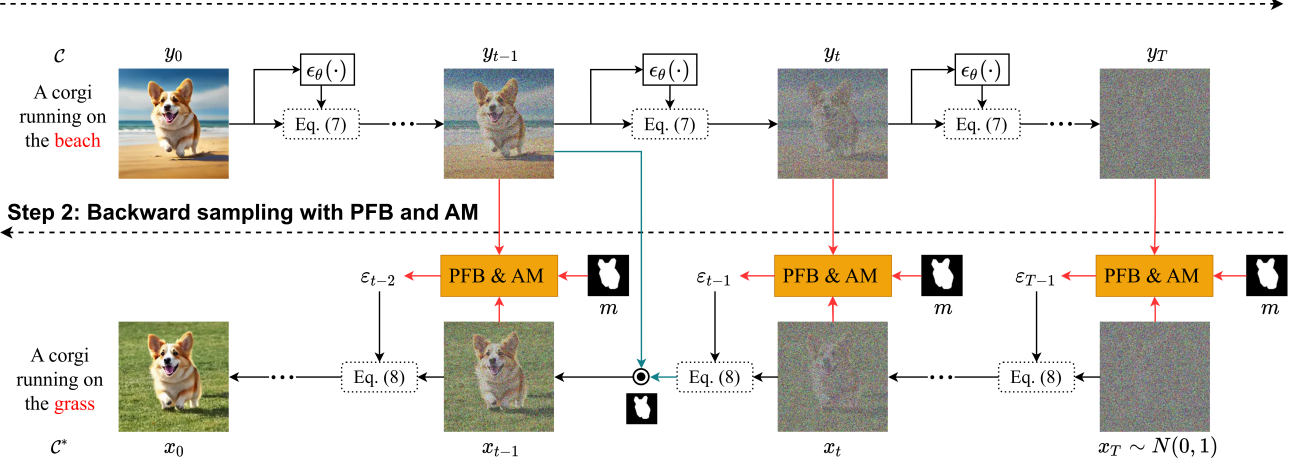


Figure 2. Pipeline of the proposed PFB-Diff framework. Our method utilizes a pre-trained diffusion model without additional training. Initially, we employ DDIM encoding to obtain noisy images y_t for all time steps. Subsequently, we perform a backward denoising process starting from a Gaussian noise x_T to generate the edited image x_0 . When estimating the noise ε_t at each time step, we adopt progressive feature blending (indicated by the red lines) to fuse the deep features of x_t and y_t . Note that we also incorporate intermediate noisy image blending (indicated by blue lines) in the early stages of the denoising process to better preserve visual details in irrelevant regions. We denote with \odot the element-wise blending of two images using the input mask m . The Eq. (7) and Eq. (8) in the figure refer to Eq. (7) in Section 3 and Eq. (8) in Section 4.1, respectively.

Eq. (5) can be written as the neural ODE, taking $\mathbf{u} = \mathbf{x}/\sqrt{\alpha}$ and $\tau = \sqrt{1/\alpha - 1}$:

$$d\mathbf{u} = \epsilon_\theta \left(\frac{\mathbf{u}}{\sqrt{1 + \tau^2}}, t \right) d\tau. \quad (6)$$

This allows us to view DDIM sampling as an Euler scheme for solving Eq. (6) with initial condition $\mathbf{u}(t = T) \sim \mathcal{N}(\mathbf{0}, \alpha_T \mathbf{I})$. As proposed by Song et al. [39], we can also use this ODE to encode an image \mathbf{x}_0 onto a latent variable \mathbf{x}_r for a timestep r , based on the assumption that the ODE process can be reversed in the limit of small steps:

$$\mathbf{x}_{t+1} = \sqrt{\frac{\alpha_{t+1}}{\alpha_t}} \mathbf{x}_t + \left(\sqrt{\frac{1}{\alpha_{t+1}} - 1} - \sqrt{\frac{1}{\alpha_t} - 1} \right) \epsilon_\theta(\mathbf{x}_t, t, C). \quad (7)$$

In other words, the diffusion process is performed in the reverse direction, that is $\mathbf{x}_0 \rightarrow \mathbf{x}_T$ instead of $\mathbf{x}_T \rightarrow \mathbf{x}_0$.

Latent diffusion models. Diffusion models often operate in the image pixel space where \mathbf{x}_0 is a sample of a real image. In this paper, we build our approach on the popular and publicly available latent diffusion model (LDM) [32]. The diffusion forward process is applied on a latent image encoding \mathbf{x}_0 and an image decoder is employed at the end of the diffusion backward process to recover \mathbf{x}_0 back to the image. For simplicity, we refer to the latent image encoding \mathbf{x}_0 as “image” in the following sections. To build more flexible conditional image generators, LDM augments the un-

derlying U-Net [33] backbone with the cross-attention [41] mechanism. The noise prediction network ϵ_θ in LDM is a U-shaped network composed of residual and transformer blocks.

4. Methods

In this section, we first give an overview of PFB-Diff (Section 4.1). We then describe two key components of our method, i.e., progressive feature blending (Section 4.2) and attention masking mechanism (Section 4.3), in detail.

4.1. An overview of our PFB-Diff framework

Given an input image \mathbf{y}_0 , along with its corresponding coarse text description d , a target text prompt d^* , and a binary mask m indicating the region of interest in the image, our objective is to generate a manipulated image \mathbf{x}_0 that fulfills the following requirements. Firstly, the entire image should be aligned with the target text prompt. Secondly, the uninterested regions should remain unaltered. Thirdly, the edited result \mathbf{x}_0 should demonstrate high consistency and quality.

To fulfill the above requirements, we propose a Progressive Feature Blending method for Diffusion-based image editing, dubbed PFB-Diff. An overview of our method is given in Figure 2. Formally, given an input image-text pair (\mathbf{y}_0, d) , a target text prompt d^* , and a binary mask m indicating the regions of interest, we first encode the text prompts d and d^* into embeddings C and C^* respectively,

using a pre-trained text encoder. Next, we sample the noisy image \mathbf{y}_t at each time step with DDIM encoding using the pre-trained diffusion model ϵ_θ . Finally, starting from a random Gaussian noise \mathbf{x}_T , we iteratively sample \mathbf{x}_t using the following equation until $t = 0$:

$$\mathbf{x}_{t-1} = \sqrt{\frac{\alpha_{t-1}}{\alpha_t}} \mathbf{x}_t + \left(\sqrt{\frac{1}{\alpha_{t-1}} - 1} - \sqrt{\frac{1}{\alpha_t} - 1} \right) \cdot \boldsymbol{\varepsilon}_{t-1}, \quad (8)$$

where $\boldsymbol{\varepsilon}_{t-1}$ represents the estimated noise at time $t - 1$. A key feature of PFB-Diff is that the text-driven blended diffusion is made not directly on the intermediate noisy images but instead on their correspondingly learned feature maps. To accomplish this, we introduce a Progressive Feature Blending (PFB) technique. Additionally, we introduce an Attention Masking (AM) mechanism for cross-attention layers, enabling text-guided generation within specific regions of interest. By incorporating both the PFB and AM into the noise prediction network ϵ_θ , we obtain the diffusion model $\hat{\epsilon}_\theta$. The $\boldsymbol{\varepsilon}_{t-1}$ in Eq. (8) is derived from $\hat{\epsilon}_\theta$ as follows,

$$\boldsymbol{\varepsilon}_{t-1} = \hat{\epsilon}_\theta(\mathbf{x}_t, t, \mathcal{C}^*, \mathbf{y}_t, \mathcal{C}, \mathbf{m}). \quad (9)$$

To further preserve the details of irrelevant regions, we also apply pixel-level blending during the early stages of the denoising process, illustrated by the blue lines in Figure 2.

4.2. Progressive Feature Blending (PFB)

To achieve localized editing, previous methods [4, 5, 9, 26, 27] employ a pixel-level blending technique, where newly generated intermediate latent variables are blended with the noised versions of the input image across different noise levels. However, empirical experiments indicate that this approach can introduce artifacts and inconsistencies in the results. This is because the pixel-level information in the intermediate noisy images lacks the necessary semantics to produce consistent and seamless fusion. While extensions have been made in latent diffusion [32], which leverages a pre-trained autoencoder to encode the input image into a lower-dimensional hidden space for efficient diffusion, the hidden space itself still lacks the essential semantics required to maintain image consistency. To address these limitations, we propose a simple yet effective module called Progressive Feature Blending (PFB). This module can be plugged into any pre-trained text-to-image frameworks to enhance their ability to generate consistent and high-quality images.

Recall that each diffusion step t contains predicting the noise $\boldsymbol{\varepsilon}$ with $(x_t, \mathcal{C}^*, \mathbf{y}_t, \mathcal{C}, \mathbf{m})$ using a U-shaped network $\hat{\epsilon}_\theta$ composed of transformer blocks. In the left branch of Figure 3, we show three consecutive blocks of the pre-trained noise prediction network ϵ_θ for \mathbf{y}_t and denote the i -th transformer block’s output as $\varphi_i(\mathbf{y}_t)$. PFB is implemented by

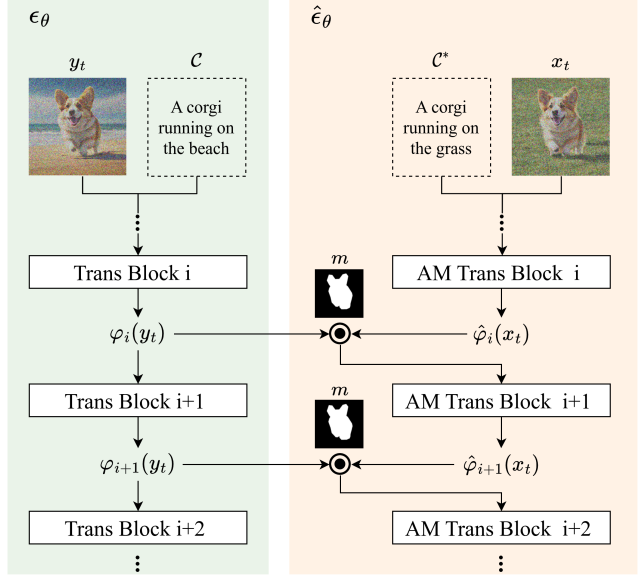


Figure 3. Progressive feature blending. The left shows the pre-trained noise prediction network $\epsilon_\theta(\cdot)$ in LDM, which is built upon U-Net [33] architecture and composed of transformer blocks. The right $\hat{\epsilon}_\theta$ is obtained by plugging progressive feature blending (PFB) and attention masking (AM) into ϵ_θ . “Trans Block i ” indicates the i -th transformer block in $\epsilon_\theta(\cdot)$. “AM Trans Block i ” indicates the i -th transformer block (equipped with attention masking) in $\hat{\epsilon}_\theta(\cdot)$. For more details of the attention masking mechanism, please refer to Section 4.3. Note that the left ϵ_θ and the right $\hat{\epsilon}_\theta$ share the same weights. We denote with \odot the element-wise blending of two feature maps using the input mask \mathbf{m} .

inserting the feature blending module into certain layers of the noise prediction network, as shown in the right branch of Figure 3. At each layer, we blend the feature map $\hat{\varphi}_i(\mathbf{x}_t)$ with $\varphi_i(\mathbf{y}_t)$ using the binary mask \mathbf{m} as below:

$$\tilde{\varphi}_i(\mathbf{x}_t) = \varphi_i(\mathbf{y}_t) \odot (1 - \mathbf{m}) + \hat{\varphi}_i(\mathbf{x}_t) \odot \mathbf{m}, \quad (10)$$

where blended feature map $\tilde{\varphi}_i(\mathbf{x}_t)$, rather than $\hat{\varphi}_i(\mathbf{x}_t)$, is fed into the next transformer block. Since the feature map size changes from block to block, we downsample or up-sample the binary mask \mathbf{m} accordingly to make the computation of Eq. (10) valid. Note that, we also modify the transformer block by incorporating an Attention Masking (AM) mechanism into the cross-attention layers, with details described in Section 4.3.

To summarize, the PFB module implements a new, feature-level text-driven blended diffusion, leading to high-quality, seamless target generation towards the guiding text prompt.

4.3. Attention Masking (AM) mechanism

When manipulating an input image from “a giraffe stands by the fence” to “a giraffe stands in the snow”, choos-

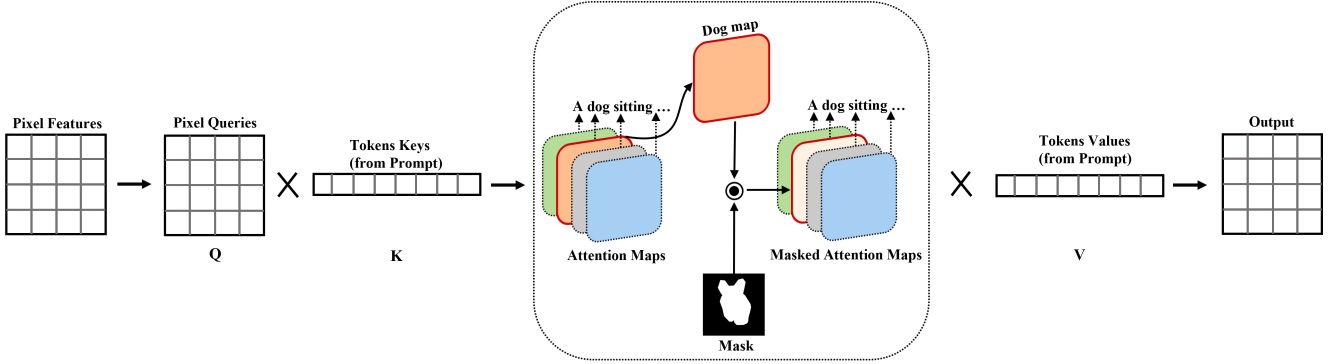


Figure 4. The details of the attention masking mechanism in the cross-attention layers. Each channel of the attention map is associated with a specific word. The channel corresponding to “dog” is corrected by a binary mask to limit the influence of “dog” to specific spatial regions on image features. We use \odot to denote element-wise multiplication.

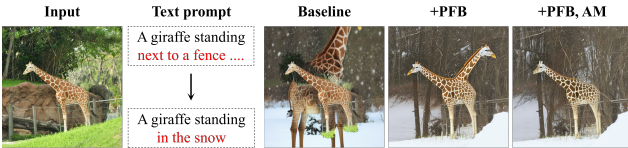


Figure 5. The role of Attention Masking (AM) in background replacement. The first column showcases a sample from the COCO dataset [24]. The second column presents the target text prompt. In the third column, without PFB and AM, previous pixel-level blending methods introduce an additional giraffe in the background. In the fourth column, by utilizing PFB, the model generates the giraffe to the desired location, but with a clear difference from the foreground instance. In the fifth column, AM ensures that the generated giraffe is faithful to the original one.

ing “snow” as the target prompt may lead to a generated image lacking global semantic consistency. Instead, we input the global text prompt “a giraffe stands in the snow” into the diffusion model to generate a new background. However, pixel-level blending cannot effectively constrain the generated giraffe to its original location. As shown in the third column (baseline) in Figure 5, blending the noised input image with newly generated content using the input binary mask can result in noticeable artifacts. While the proposed progressive feature blending helps to restrict the generated giraffe to desired regions, as shown in the fourth column of Figure 5, the model still sometimes produces unwanted artifacts around the foreground giraffe.

Masking the attention maps of specific words is introduced to address this issue. As mentioned in Figure 3, we present an Attention Masking (AM) mechanism to fuse the visual features with the textual ones. The details of the attention masking mechanism are provided in Figure 4. Specifically, the deep spatial features of the noisy image are projected to a query matrix Q , and the text prompt’s embedding is projected to a key matrix K and a value matrix

V via learned linear projections. The attention score map is computed by

$$M = (QK^T / \sqrt{n}), \quad (11)$$

where n is the latent projection dimension. Given the binary mask \mathbf{m} , the attention score maps is rectified by

$$\widehat{M}_{ij}^k = \begin{cases} M_{ij}^k, & \mathbf{m}_{ij}^k = 1, \\ -inf, & \mathbf{m}_{ij}^k = 0, \end{cases} \quad (12)$$

where the entry M_{ij}^k of the matrix M gives the weight of the value of the k -th textual token at the position (i, j) . Finally, the output of the masked cross-attention layer is defined as

$$\mathcal{F} = \text{softmax}(\widehat{M})V. \quad (13)$$

By utilizing the masked attention maps, the model can effectively limit the impact of each word to specific spatial regions on the image features. As a result, the model can enforce the generation of the target objects to desired positions and shapes.

5. Experiments

5.1. Experimental setup

Dataset We conduct experimental evaluations on two datasets. We first construct a dataset composed of synthetic images generated by Midjourney¹, a highly popular text-to-image model. We have designed more than 50 text prompts with relatively simple descriptions, such as “a happy corgi running on the beach.” These prompts take into account various factors, including the number of objects, image style, object attributes, secondary objects, and spatial relationships between objects, allowing us to evaluate the performance of editing methods in diverse scenarios. We conduct most qualitative experiments on this dataset in order

¹<https://www.midjourney.com/home/?callbackUrl=%2Fapp%2F>

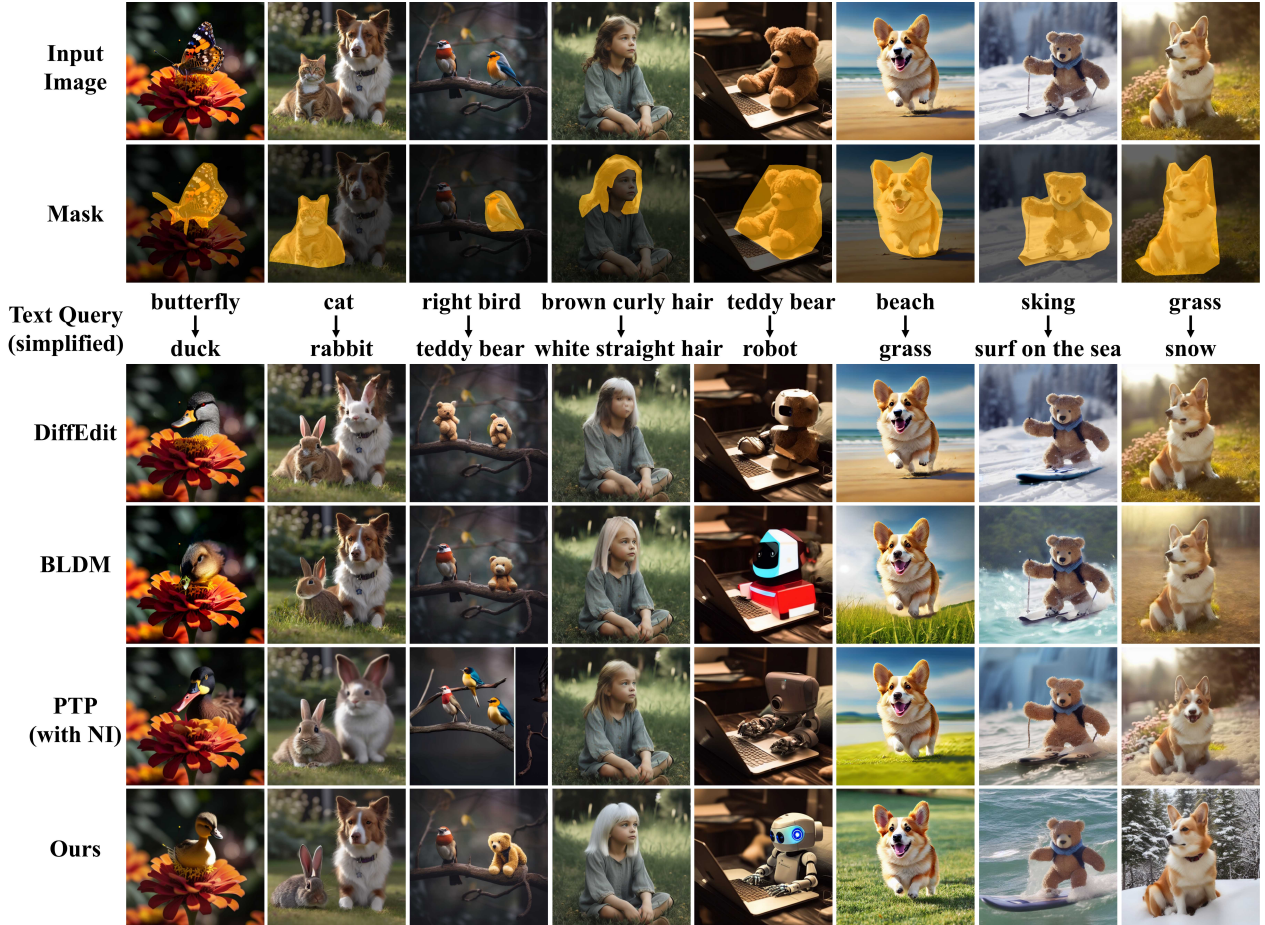


Figure 6. Examples of edits on images obtained from Midjourney. For mask-based methods (BLDM [5], Ours), we use the manually annotated rough labels shown in the second row. For object/background replacement, both DiffEdit [9] and our method employ a 100% encoding rate during DDIM encoding.

to evaluate edits that involve changing the background, replacing objects, or changing object properties. To evaluate edits based on more complex text prompts and conduct quantitative comparisons, we collect 9,850 images from the COCO dataset [24] to build the COCO-animals-10k dataset, or COCOA-10k for short. The images in the dataset contain objects from 9 specific classes: dogs, cats, sheep, cows, horses, birds, elephants, zebras, and giraffes. By appropriately modifying the captions of the images, COCOA-10k can be used to evaluate foreground object replacement and background editing. Please refer to the Appendix for further details.

Diffusion models In our experiments, we use the pre-trained latent diffusion models [32] as the backbone. We evaluate the text-driven editing on 890M parameter text-conditional model trained on LAION-5B [36], known as stable diffusion [32], at 512×512 resolution. We use 50 steps in DDIM sampling [39] with a fixed schedule to gen-

erate images, which allows within 13 seconds on a single TITAN V GPU. Besides, we follow [9] and use DDIM encoding to obtain intermediate noisy images of the input image. For more details, please refer to the Appendix.

Compared baselines We compare our method with three state-of-the-art text-driven editing approaches, including mask-based methods such as BLDM [4], and mask-free methods such as DiffEdit [9] and Prompt-to-Prompt [15]. Note that Prompt-to-Prompt cannot be directly applied to edit real images. Null-text inversion [28] provides a technique for inverting input images and enables the text editing technique of Prompt-to-Prompt on real images. Therefore, we adopt the Null-text inversion approach to invert the images and subsequently utilize Prompt-to-Prompt for editing purposes. For a fair comparison, we adopt Stable Diffusion v1-4 as the pre-trained text-to-image model for all the compared methods.

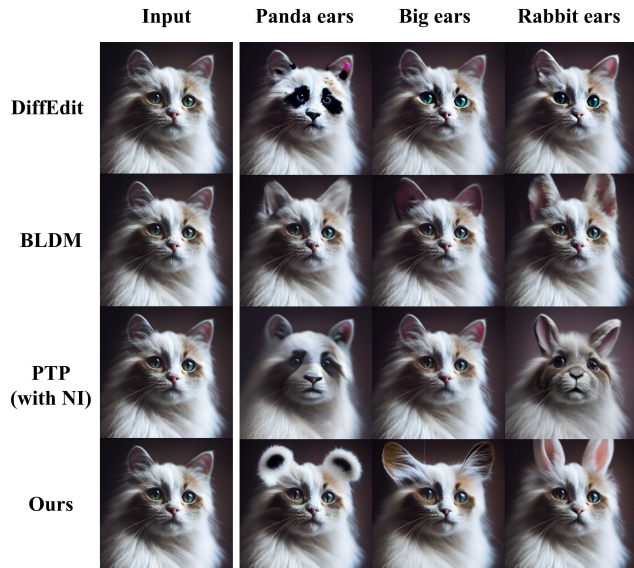


Figure 7. Qualitative comparisons on cat ears editing. Our method can produce ears that match text prompts while others cannot.

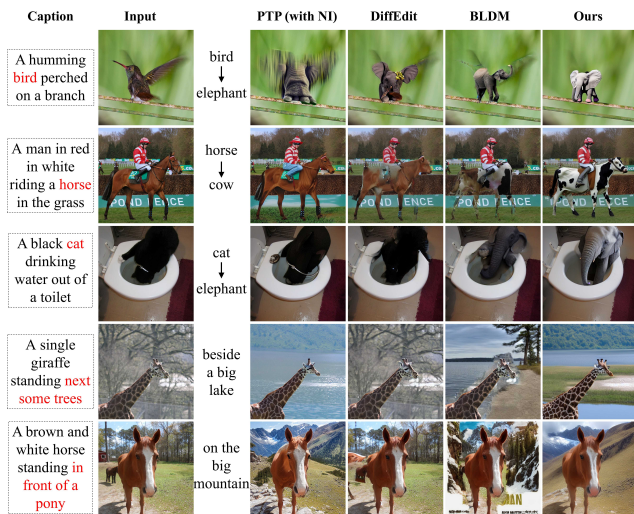


Figure 8. Examples of edits on COCO [24] images.

Evaluation metrics Text-based semantic image editing requires meeting both requirements: 1) the generated image needs to align with the text prompts, and 2) the generated image needs to maintain high quality and realism. To measure these two aspects, we utilize the following four metrics to evaluate the generated images: 1) FID score [16], which is a widely used metric for evaluating the quality of generated images. Note that we follow [23] and use the CLIP [30] model to extract features for calculating the FID score. 2) CLIP score [30], which evaluates the alignment between guided text prompts and edited images. A higher CLIP score indicates better matching to the text descrip-

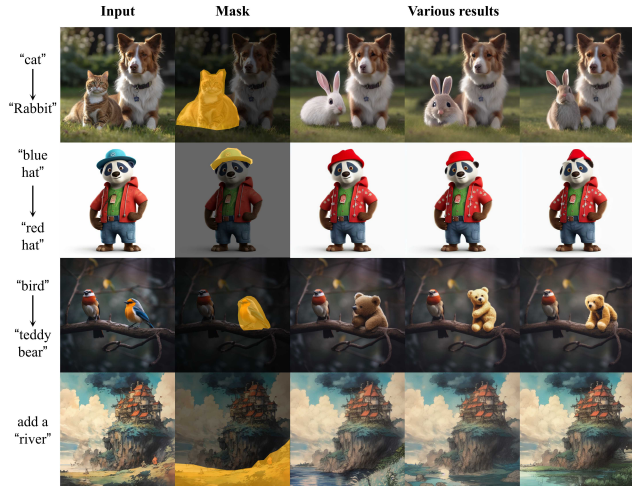


Figure 9. Our framework can synthesize realistic and diverse results according to the same source image and guided text prompt.

tions. 3) Local CLIP score, which evaluates the similarity between the local edit region and the target object. 4) Local FID score, which calculates FID on local regions. Since a single object occupies a small area in an image and corresponds to a single word in the text description, the global CLIP score cannot well reflect the quality of object replacement. To address this, we introduce Local CLIP, which concentrates on specific object regions by cropping images using bounding boxes. In the case of replacing a dog with a horse, we crop the target region from the edited image and evaluate its similarity to the text prompt "a horse". Similarly, the global FID cannot well reflect the realism of local generations, thus we introduce local FID to measure FID in the local regions.

5.2. Qualitative results

Figure 6 visualizes object and background editing on images generated by Midjourney². In comparison with other methods, PFB-Diff generally performs more targeted and accurate edits, leaving irrelevant regions intact and maintaining high image quality. By operating on deep features with rich semantics, our approach takes into account semantic consistency in the edited results. For instance, the pose of the teddy bear in the third column and the gesture of the robot in the fifth column are both adapted to fit their respective scenes. DiffEdit [9] and PTP [15] can cause undesired modifications and perform poorly when an image contains multiple objects. Additionally, DiffEdit struggles to generate desired scenes in background replacement. Although BLDM [4] can accurately generate content aligned well with text prompts, it often lacks semantic consistency

²<https://www.midjourney.com/home/?callbackUrl=%2Fapp%2F>

Table 1. Quantitative comparison of different methods for object replacement and background replacement on 9,843 and 1,579 COCO [24] animal images, respectively. Local-CLIP score represents the CLIP score calculated only in the region of the target object. Please refer to Section 5.1 for more details. (Bold indicates the best result, blue indicates the second-best result.)

Methods	Object				Background	
	CLIP Score \uparrow	FID \downarrow	Local-CLIP \uparrow	Local-FID \downarrow	CLIP Score \uparrow	FID \downarrow
PTP [15]	30.33	9.587	24.62	12.08	31.55	13.92
BLDM [4]	29.95	6.143	25.31	9.630	30.38	20.44
DiffEdit [9]	29.30	3.780	22.38	6.147	26.92	1.741
Ours-obj	30.36	6.259	25.45	9.274	/	/
Ours-dst	30.81	5.935	24.84	8.935	32.25	13.77

in edited results. Figure 7 further demonstrates the effectiveness of our method on editing only a part of an object, where only PFB-Diff can precisely modify the style of cat ears, while other methods cannot.

Similar observations can be found in real image editing. Figure 8 shows the results on COCOA-10k dataset. The complex scenes and text descriptions in COCOA-10k dataset make it a good benchmark for evaluating generalization ability. Moreover, the masks in COCOA-10k are often incompatible with the target text prompts (e.g., the model is expected to generate a cat in an area shaped like a giraffe), allowing us to evaluate the robustness of mask-based methods to extreme masks. Even under such extreme masks, our method can still generate desired content while maintaining high quality and consistency. In contrast, other baselines either fail to generate desired objects/scenes or produce unwanted artifacts.

Mask-based models can achieve satisfactory performance in background replacement by utilizing precise masks available in datasets like COCO [24]. However, such precise segmentation is not commonly available in real-world scenarios. In practice, users often provide rough masks, leading to foreground objects being segmented along with some original background information. For instance, when separating a horse from the grass, the extracted mask will inevitably include some portions of the surrounding grass. To assess the effectiveness of mask-based methods in practical settings, we provide dilated masks to these models. As illustrated, while BLDM [4] successfully replaces the background, there are remnants of the old background content along the boundaries, resulting in an unnatural fusion. In contrast, PFB-Diff effectively eliminates the interference of the old background associated with the mask, enabling a seamless fusion between the new scene and the foreground object. This demonstrates the ability of PFB-Diff to overcome challenges posed by imperfect masks and achieve superior results in terms of realistic background

replacement.

Among the evaluated methods, only PFB-Diff can simultaneously meet the requirements of high accuracy, high image quality, seamless fusion, and irrelevance preservation, in both object and background editing. Figure 9 shows that the proposed method can generate a variety of plausible outcomes. More qualitative results can be found in the Appendix.

5.3. Quantitative analysis

For quantitative comparison, we conduct object/background editings on 9,843 images of the COCOA-10k dataset. For PTP [15], DiffEdit [9], and Ours+dst, the input data structure is a triplet consisting of an image, description, and target text prompt, while the target text prompt is replaced with a guided category (e.g., a dog) for BLDM [4] and Ours+obj. For object editing, we replace words indicating animal categories in image descriptions with other categories to construct target text prompts. For background replacement, we select 1,597 images containing the word “standing” from the COCOA-10k dataset and replace the context after “standing” with random scenes, such as on the beach, in the snow, on the grass, or on a dusty road. Figure 8 visualizes some examples of the COCOA-10k dataset.

Quantitative results on object editing and background editing are presented in Table 1. Overall, our method achieves the highest CLIP score and Local CLIP score, while ranking second in FID and Local FID. These results demonstrate that our method enables more precise and targeted editing while maintaining image realism. DiffEdit often fails to produce modifications to the original image, resulting in minimal changes and, therefore, obtaining the best FID scores but the worst CLIP scores. As discussed in Section 5.1, the global CLIP score may not accurately reflect the precision of local object editing. Consequently, while DiffEdit [9] achieves a similar CLIP score to other

Table 2. Human evaluation on semantic image editing. 1 is the worst, 4 is the best. Users rated ours as the best editing results.

Method	PTP [15]	BLDM [4]	DiffEdit [9]	Ours
Score \uparrow	2.10	2.47	1.72	3.78

baselines in Table 1, its local CLIP score is significantly lower than others.

5.4. User study

To quantify overall human satisfaction, we conduct a user study on 28 participants. In the study, we use 30 groups of images, each group contains one input and four outputs. All these results in each group are presented side-by-side to participants. These 30 groups cover various editing tasks, including object replacement, background replacement, and object property editing. The input images include both real images and images generated by Midjourney. Participants are given unlimited time to rank the score from 1 to 4 (4 is the best, 1 is the worst) simultaneously considering the alignment with text prompts, realism, and faithfulness to the original input. We report the average ranking score in Table 2. We observe that users prefer our results more than others.

5.5. Ablation studies

Our model consists of two pivotal components: the Progressive Feature Blending (PFB) technique and the Attention Masking (AM) mechanism. In this section, we validate their effectiveness. To this end, we construct two variant models: 1) *Baseline*, which adopts the pixel-blending method utilized by previous works [9]. 2) *Baseline + PFB*, which incorporates the PFB module. *Baseline + PFB* is equivalent to removing the attention masking mechanism from PFB-Diff.

Table 3 presents the quantitative comparisons on background editing. Overall, our method gains the best CLIP score. While the baseline method gains the best FID score, it often generates an unnatural blend of the original foreground objects and the newly generated background, as shown in Figure 10. When we add PFB to the baseline, image fusion becomes more seamless and natural.

During background replacement, the results obtained from *Baseline + PFB* often exhibit additional objects around the foreground objects. As shown in the fourth row and first column of Figure 10, another horse appears around the original horse. When generating the new background, diffusion models are fed with the text prompt “a horse is standing on a dusty road”, but Baseline+PFB fails to restrict the generated horse to the position of the original horse. Masking the attention maps of specific words is introduced

Table 3. Quantitative comparison of different variants of our method. We evaluate the background editing performance on 1,579 COCO [24] animal images. PFB-Diff achieves the best CLIP score and Local CLIP score by leveraging all the proposed techniques.

Method	CLIP Score \uparrow	FID \downarrow	Local-CLIP \uparrow
Baseline	31.3	12.0	28.19
+PFB	31.9	13.0	29.86
+PFB, AM	32.3	13.4	30.12

to address this issue. As shown in the last row of Figure 10, when we reintroduced AM in the model, we could observe a significant improvement in the aforementioned problems. We can also observe that AM has little influence on foreground object replacement.

6. Limitations and Future Work

While our method has achieved good results, our method requires the user to provide a mask to indicate the interested regions. Compared with the mask-free method, the mask-based method can often provide more accurate editing, but it can also cause inconvenience in some scenarios. Compared with previous mask-based methods, our method can still achieve good performance even if the user provides a coarse mask. Even fed with extreme masks, such as generating a horse in a bird-shaped mask, PFB-Diff can still obtain good results. Another limitation is that our method cannot be applied to style transfer. We will solve these problems in our future work.

7. Conclusion

This paper introduced PFB-Diff, a novel progressive feature blending method designed for diffusion-based image editing. By seamlessly blending irrelevant content with newly generated content across multiple levels of features, our approach achieves more natural and coherent editing results. Furthermore, we incorporate masked cross-attention maps to restrict the influence of specific words on the target area, resulting in enhanced performance. Through empirical experiments on both real images and those generated by large-scale text-to-image models, we demonstrated the superior performance of our method compared to existing state-of-the-art techniques. Our approach effectively addresses various editing tasks, including object/background replacement and changing object properties, while preserving high-quality results and maintaining accurate image-text alignments. Notably, our proposed method exhibits high efficiency, as it does not require fine-tuning or training. Both the PFB and AM modules are plug-and-play and



Figure 10. Ablation study on the effects of the two modules of our method. Examples of edits on COCO [24] images are reported.

can be easily adapted to any pre-trained text-to-image diffusion models. The above advantages position PFB-Diff as a promising direction for future research in text-driven image editing.

References

- [1] Rameen Abdal, Yipeng Qin, and Peter Wonka. Image2stylegan: How to embed images into the stylegan latent space? In *Proceedings of the IEEE international conference on computer vision*, pages 4432–4441, 2019. 2
- [2] Rameen Abdal, Yipeng Qin, and Peter Wonka. Image2stylegan++: How to edit the embedded images? In *Proceedings of the IEEE/CVF Conference on Computer Vision and Pattern Recognition*, pages 8296–8305, 2020. 2
- [3] Rameen Abdal, Peihao Zhu, John Femiani, Niloy Mitra, and Peter Wonka. Clip2stylegan: Unsupervised extraction of stylegan edit directions. In *ACM SIGGRAPH 2022 conference proceedings*, pages 1–9, 2022. 3
- [4] Omri Avrahami, Ohad Fried, and Dani Lischinski. Blended latent diffusion. *arXiv preprint arXiv:2206.02779*, 2022. 2, 3, 5, 7, 8, 9, 10, 13, 14, 16, 17, 18
- [5] Omri Avrahami, Dani Lischinski, and Ohad Fried. Blended diffusion for text-driven editing of natural images. In *Proceedings of the IEEE/CVF Conference on Computer Vision and Pattern Recognition*, pages 18208–18218, 2022. 2, 3, 5,

- [6] David Bau, Alex Andonian, Audrey Cui, YeonHwan Park, Ali Jahanian, Aude Oliva, and Antonio Torralba. Paint by word. *arXiv preprint arXiv:2103.10951*, 2021. [3](#)
- [7] Mikołaj Bińkowski, Danica J Sutherland, Michael Arbel, and Arthur Gretton. Demystifying mmd gans. *arXiv preprint arXiv:1801.01401*, 2018.
- [8] Jooyoung Choi, Sungwon Kim, Yonghyun Jeong, Youngjune Gwon, and Sungroh Yoon. Ilvr: Conditioning method for denoising diffusion probabilistic models. *arXiv preprint arXiv:2108.02938*, 2021. [3](#)
- [9] Guillaume Couairon, Jakob Verbeek, Holger Schwenk, and Matthieu Cord. Diffedit: Diffusion-based semantic image editing with mask guidance. In *The Eleventh International Conference on Learning Representations*, 2023. [2](#), [3](#), [5](#), [7](#), [8](#), [9](#), [10](#), [13](#), [14](#), [16](#)
- [10] Prafulla Dhariwal and Alexander Nichol. Diffusion models beat gans on image synthesis. *Advances in Neural Information Processing Systems*, 34:8780–8794, 2021. [1](#)
- [11] Patrick Esser, Robin Rombach, and Bjorn Ommer. Taming transformers for high-resolution image synthesis. In *Proceedings of the IEEE/CVF conference on computer vision and pattern recognition*, pages 12873–12883, 2021.
- [12] Rinon Gal, Yuval Alaluf, Yuval Atzmon, Or Patashnik, Amit H Bermano, Gal Chechik, and Daniel Cohen-Or. An image is worth one word: Personalizing text-to-image generation using textual inversion. *arXiv preprint arXiv:2208.01618*, 2022. [2](#), [3](#)
- [13] Rinon Gal, Or Patashnik, Haggai Maron, Amit H Bermano, Gal Chechik, and Daniel Cohen-Or. Stylegan-nada: Clip-guided domain adaptation of image generators. *ACM Transactions on Graphics (TOG)*, 41(4):1–13, 2022. [3](#)
- [14] Ian Goodfellow, Jean Pouget-Abadie, Mehdi Mirza, Bing Xu, David Warde-Farley, Sherjil Ozair, Aaron Courville, and Yoshua Bengio. Generative adversarial nets. *Advances in neural information processing systems*, 27, 2014. [2](#)
- [15] Amir Hertz, Ron Mokady, Jay Tenenbaum, Kfir Aberman, Yael Pritch, and Daniel Cohen-Or. Prompt-to-prompt image editing with cross attention control. *arXiv preprint arXiv:2208.01626*, 2022. [3](#), [7](#), [8](#), [9](#), [10](#), [13](#), [14](#)
- [16] Martin Heusel, Hubert Ramsauer, Thomas Unterthiner, Bernhard Nessler, and Sepp Hochreiter. Gans trained by a two time-scale update rule converge to a local nash equilibrium. *Advances in neural information processing systems*, 30, 2017. [8](#)
- [17] Jonathan Ho, Ajay Jain, and Pieter Abbeel. Denoising diffusion probabilistic models. *Advances in Neural Information Processing Systems*, 33:6840–6851, 2020. [1](#), [3](#)
- [18] Erik Härkönen, Aaron Hertzmann, Jaakko Lehtinen, and Sylvain Paris. Ganspace: Discovering interpretable gan controls. In *Proc. NeurIPS*, 2020. [2](#), [3](#)
- [19] Tero Karras, Samuli Laine, and Timo Aila. A style-based generator architecture for generative adversarial networks. In *Proceedings of the IEEE/CVF Conference on Computer Vision and Pattern Recognition*, pages 4401–4410, 2019. [2](#), [3](#)
- [20] Tero Karras, Samuli Laine, Miika Aittala, Janne Hellsten, Jaakko Lehtinen, and Timo Aila. Analyzing and improving the image quality of stylegan. In *Proceedings of the IEEE/CVF Conference on Computer Vision and Pattern Recognition*, pages 8110–8119, 2020. [2](#), [3](#)
- [21] Bahjat Kawar, Shiran Zada, Oran Lang, Omer Tov, Huiwen Chang, Tali Dekel, Inbar Mosseri, and Michal Irani. Imagic: Text-based real image editing with diffusion models. *arXiv preprint arXiv:2210.09276*, 2022. [2](#), [3](#)
- [22] Gwanghyun Kim, Taesung Kwon, and Jong Chul Ye. Diffusionclip: Text-guided diffusion models for robust image manipulation. In *Proceedings of the IEEE/CVF Conference on Computer Vision and Pattern Recognition*, pages 2426–2435, 2022. [3](#)
- [23] Tuomas Kynkäänniemi, Tero Karras, Miika Aittala, Timo Aila, and Jaakko Lehtinen. The role of imagenet classes in fr\`echet inception distance. *arXiv preprint arXiv:2203.06026*, 2022. [8](#)
- [24] Tsung-Yi Lin, Michael Maire, Serge Belongie, James Hays, Pietro Perona, Deva Ramanan, Piotr Dollár, and C Lawrence Zitnick. Microsoft coco: Common objects in context. In *Computer Vision–ECCV 2014: 13th European Conference, Zurich, Switzerland, September 6–12, 2014, Proceedings, Part V 13*, pages 740–755. Springer, 2014. [6](#), [7](#), [8](#), [9](#), [10](#), [11](#), [14](#), [17](#), [18](#)
- [25] Cheng Lu, Yuhao Zhou, Fan Bao, Jianfei Chen, Chongxuan Li, and Jun Zhu. DPM-solver: A fast ODE solver for diffusion probabilistic model sampling in around 10 steps. In Alice H. Oh, Alekh Agarwal, Danielle Belgrave, and Kyunghyun Cho, editors, *Advances in Neural Information Processing Systems*, 2022. [13](#)
- [26] Andreas Lugmayr, Martin Danelljan, Andres Romero, Fisher Yu, Radu Timofte, and Luc Van Gool. Repaint: Inpainting using denoising diffusion probabilistic models. In *Proceedings of the IEEE/CVF Conference on Computer Vision and Pattern Recognition*, pages 11461–11471, 2022. [3](#), [5](#)
- [27] Chenlin Meng, Yutong He, Yang Song, Jiaming Song, Jiajun Wu, Jun-Yan Zhu, and Stefano Ermon. Sdedit: Guided image synthesis and editing with stochastic differential equations. In *International Conference on Learning Representations*, 2021. [2](#), [3](#), [5](#), [13](#)
- [28] Ron Mokady, Amir Hertz, Kfir Aberman, Yael Pritch, and Daniel Cohen-Or. Null-text inversion for editing real images using guided diffusion models. In *Proceedings of the IEEE/CVF Conference on Computer Vision and Pattern Recognition*, pages 6038–6047, 2023. [3](#), [7](#), [14](#), [16](#)
- [29] Alex Nichol, Prafulla Dhariwal, Aditya Ramesh, Pranav Shyam, Pamela Mishkin, Bob McGrew, Ilya Sutskever, and Mark Chen. Glide: Towards photorealistic image generation and editing with text-guided diffusion models. *arXiv preprint arXiv:2112.10741*, 2021. [1](#)
- [30] Alec Radford, Jong Wook Kim, Chris Hallacy, Aditya Ramesh, Gabriel Goh, Sandhini Agarwal, Girish Sastry, Amanda Askell, Pamela Mishkin, Jack Clark, et al. Learning transferable visual models from natural language supervision. In *International conference on machine learning*, pages 8748–8763. PMLR, 2021. [3](#), [8](#)

- [31] Aditya Ramesh, Mikhail Pavlov, Gabriel Goh, Scott Gray, Chelsea Voss, Alec Radford, Mark Chen, and Ilya Sutskever. Zero-shot text-to-image generation. In *International Conference on Machine Learning*, pages 8821–8831. PMLR, 2021. 1, 3
- [32] Robin Rombach, Andreas Blattmann, Dominik Lorenz, Patrick Esser, and Björn Ommer. High-resolution image synthesis with latent diffusion models. In *Proceedings of the IEEE/CVF Conference on Computer Vision and Pattern Recognition*, pages 10684–10695, 2022. 1, 3, 4, 5, 7
- [33] Olaf Ronneberger, Philipp Fischer, and Thomas Brox. U-net: Convolutional networks for biomedical image segmentation. In *Medical Image Computing and Computer-Assisted Intervention–MICCAI 2015: 18th International Conference, Munich, Germany, October 5–9, 2015, Proceedings, Part III 18*, pages 234–241. Springer, 2015. 4, 5, 14
- [34] Nataniel Ruiz, Yuanzhen Li, Varun Jampani, Yael Pritch, Michael Rubinstein, and Kfir Aberman. Dreambooth: Fine tuning text-to-image diffusion models for subject-driven generation. *arXiv preprint arXiv:2208.12242*, 2022. 2, 3
- [35] Chitwan Saharia, William Chan, Saurabh Saxena, Lala Li, Jay Whang, Emily L Denton, Kamyar Ghasemipour, Raphael Gontijo Lopes, Burcu Karagol Ayan, Tim Salimans, et al. Photorealistic text-to-image diffusion models with deep language understanding. *Advances in Neural Information Processing Systems*, 35:36479–36494, 2022. 1, 3
- [36] Christoph Schuhmann, Romain Beaumont, Richard Vencu, Cade W Gordon, Ross Wightman, Mehdi Cherti, Theo Coombes, Aarush Katta, Clayton Mullis, Mitchell Wortsman, et al. Laion-5b: An open large-scale dataset for training next generation image-text models. In *Thirty-sixth Conference on Neural Information Processing Systems Datasets and Benchmarks Track*. 7
- [37] Yujun Shen, Jinjin Gu, Xiaou Tang, and Bolei Zhou. Interpreting the latent space of gans for semantic face editing. In *Proceedings of the IEEE/CVF Conference on Computer Vision and Pattern Recognition*, pages 9243–9252, 2020. 2
- [38] Jascha Sohl-Dickstein, Eric Weiss, Niru Maheswaranathan, and Surya Ganguli. Deep unsupervised learning using nonequilibrium thermodynamics. In *International Conference on Machine Learning*, pages 2256–2265. PMLR, 2015. 3
- [39] Jiaming Song, Chenlin Meng, and Stefano Ermon. Denoising diffusion implicit models. In *International Conference on Learning Representations*, 2021. 3, 4, 7, 13
- [40] Yang Song and Stefano Ermon. Improved techniques for training score-based generative models. *Advances in neural information processing systems*, 33:12438–12448, 2020. 3
- [41] Ashish Vaswani, Noam Shazeer, Niki Parmar, Jakob Uszkoreit, Llion Jones, Aidan N Gomez, Łukasz Kaiser, and Illia Polosukhin. Attention is all you need. *Advances in neural information processing systems*, 30, 2017. 4
- [42] Zongze Wu, Dani Lischinski, and Eli Shechtman. Stylespace analysis: Disentangled controls for stylegan image generation. In *Proceedings of the IEEE/CVF Conference on Computer Vision and Pattern Recognition*, pages 12863–12872, 2021. 2
- [43] Ceyuan Yang, Yujun Shen, and Bolei Zhou. Semantic hierarchy emerges in deep generative representations for scene synthesis. *International Journal of Computer Vision*, pages 1–16, 2021. 2
- [44] Zhixing Zhang, Ligong Han, Arnab Ghosh, Dimitris Metaxas, and Jian Ren. Sine: Single image editing with text-to-image diffusion models. *arXiv preprint arXiv:2212.04489*, 2022. 2
- [45] Jiapeng Zhu, Yujun Shen, Deli Zhao, and Bolei Zhou. In-domain gan inversion for real image editing. In *European Conference on Computer Vision*, pages 592–608. Springer, 2020. 2

A. Implementation details of the compared methods

For Blended Latent Diffusion³ (shorted as BLDM) [4], Prompt-to-Prompt⁴ [15] (shorted as PTP), we adopt their official implementations.

DiffEdit [9] does not have an official implementation, whereas Lu et al. [25] released a popular re-implementation⁵ of DiffEdit in their paper. To accelerate the sampling, they use the dpm-solver [25] sampling method in their implementation instead of DDIM [39] sampling used in the original paper of DiffEdit. To make a full re-implementation of DiffEdit, we slightly modified Lu’s re-implementation and use the DDIM sampling method mentioned in the original paper.

We also conduct a comparison with mask-based DiffEdit, abbreviated as DiffEdit + Mask, where we replace their self-predicted masks with user-provided masks. This variant essentially degenerates DiffEdit to SDEdit [27] + DDIM encoding, which serves as our baseline. In simple terms, SDEdit [27] + DDIM encoding is equivalent to PFB-Diff without progressive feature blending and masked attention, and also equivalent to DiffEdit without mask inference.

For a fair comparison, we adopt stable-diffusion-v1-4 as the pre-trained text-to-image model for all the compared methods.

B. Experiment details

B.1. COCO-animals-10k dataset

To quantitatively evaluate the performance of text-based image editing, we create a dataset called COCO-animals-10k, abbreviated as COCOA-10k. Specifically, we collect 9,850 images from the COCO dataset that include objects from 10 specific classes: dogs, cats, sheep, cows, horses, birds, elephants, zebras, giraffes, and bears. By appropriately modifying the captions of the images, this dataset

³<https://github.com/omriav/blended-latent-diffusion>

⁴<https://github.com/google/prompt-to-prompt>

⁵<https://github.com/LuChengTHU/dpm-solver>

can be used to evaluate foreground object replacement and background editing. To assess foreground object replacement, we substitute animal-related words in the image captions with words representing diverse animal categories. For background replacement, we select 1,597 images from the COCOA-10k dataset that include the term “standing”. Next, we replace the text descriptions following “standing” with random scenes, such as being on a beach, in the snow, on grass, on a big mountain, on a dusty road, or in a desert area. Figure 14 & 15 visualize some examples of the COCOA-10k dataset.

B.2. Details of PFB-Diff

Given an input image, we first utilize DDIM encoding to obtain intermediate noisy images, represented as \mathbf{y}_t in Figure 2 of the manuscript. Afterward, we perform the reverse denoising process from a randomly generated Gaussian noise \mathbf{x}_T and progressively denoise it.

When estimating noise at each time step, we incorporate progressive feature blending (PFB) and attention masking (AM) in specific layers of the noise prediction model $\epsilon_\theta(\cdot)$. The model follows a U-Net [33] architecture consisting of 13 layers, each comprising a residual block and a transformer block. Progressive feature blending is applied from layers 8 to 13 while attention masking is employed from layers 4 to 13.

Furthermore, to enhance the faithfulness to the original images, we combine our approach with pixel-level blending during the early stages of the denoising process. This involves blending the noisy image \mathbf{y}_t with the generated latent variable \mathbf{x}_t . For foreground replacement, we apply pixel-level blending during the first 50% of the timesteps, while for background replacement, it is applied for the first 20% timesteps.

Due to the imprecise nature of user-provided masks, there is often a challenge in accurately segmenting foreground objects without including parts of the background. For instance, when separating a horse from the grass, the extracted mask will inevitably include some portions of the surrounding grass. To address this issue during background replacement, we remove progressive feature blending (PFB) and attention masking (AM) during the last 20% of the timesteps.

C. More analysis of PFB-Diff

Figure 11 shows some failure cases of our method. Our method can generate images from random noise. We fix the target text prompt and the input image. Then, we randomly sample 20 results. As shown in Figure 11, sometimes unwanted dog fur appears around the original dog in background replacement. Besides, the rabbit does not have a body in only one case.



Figure 11. Failure cases. Unwanted hair appears around the dog in background replacement.

In Figure 12, we visualize the impact of timesteps we apply pixel-level blending and the number of layers we apply PFB. In general, applying PFB to the low-level feature map (layers 4-13) will keep too much redundant information, such as the information of the old background (e.g., the grass around the dog). However, if it is only applied to very high-level features (layers 10-13), the detailed information of the irrelevant area (the foreground dog) will be lost. Meanwhile, applying pixel-level blending at more timesteps (50% timesteps) will retain more details of the original image. As shown in Figure 12, applying PFB at layers 8-13 and applying pixel-level blending for the first 20% of time steps is a good choice for background editing.

D. More qualitative results

Figure 13 illustrates editing examples on images generated by Midjourney⁶, in comparison with both mask-free editing methods, i.e., DiffEdit [9] and Prompt-to-Prompt [15] (with Null-text Inversion [28]), as well as mask-based editing methods, i.e., BLDM [4]. PFB-Diff generally performs more targeted and accurate edits, leaving irrelevant regions intact. Consider for example the third column of Figure 13, where PFB-Diff can accurately produce a red hat, while other methods fail to generate a hat of specified colors.

Additional qualitative examples of editings on COCO [24] images are shown in Figure 14 (object replacement) and Figure 15 (background replacement).

⁶<https://www.midjourney.com/home/?callbackUrl=%2Fapp%2F>

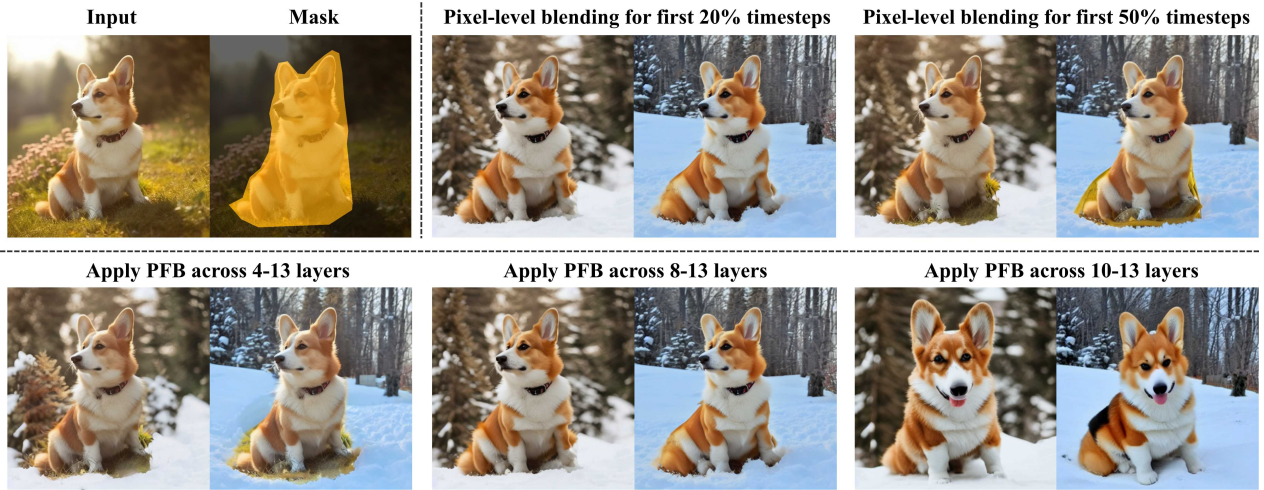


Figure 12. Illustration of the influence of some hyper-parameters in background editing. We randomly sample two initial Gaussian noises and fix them as the starting point for the denoising process under different hyper-parameter settings. Each pair showcases the editing results starting from these initial noises conditioned on “a dog sitting on snow.”









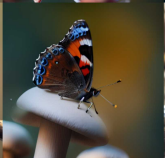




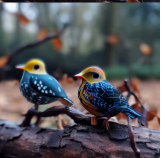

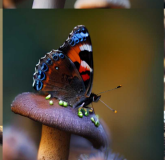




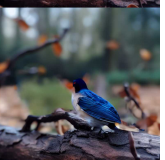

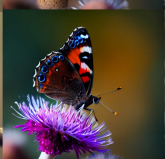

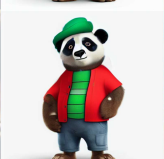


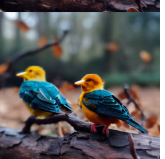

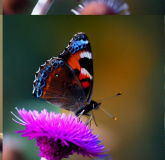




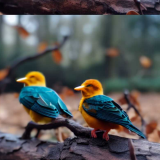

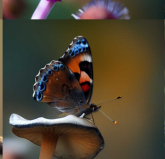




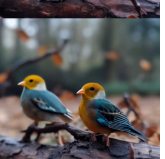
Input text prompt	A bird and another bird standing on a branch	A photo of a butterfly on a flower	A children is drawing a castle next to the river	A panda wearing a blue hat green shirt and blue pan	A happy corgi running on the beach	A cat wearing blue shirt	Two lego birds sitting on a branch
Target text prompt	A bird and an owl standing on a branch	A photo of a butterfly on a mushroom	A children is drawing a pencil drawing of a river next to the river	A panda wearing a red hat green shirt and blue pan	A happy corgi running on the road	A cat wearing nothing	Two real birds sitting on a branch
Input							
PTP (with NI)							
BLDM							
DiffEdit							
DiffEdit +Mask							
Ours							

Figure 13. More qualitative comparisons on images generated by Midjourney. We compare our method with BLDM [4], PTP (with Null-text Inversion [28]), and DiffEdit [9] on various editing tasks, including object replacement (columns 1-4), background editing (column 5), and object property editing (columns 6-7).

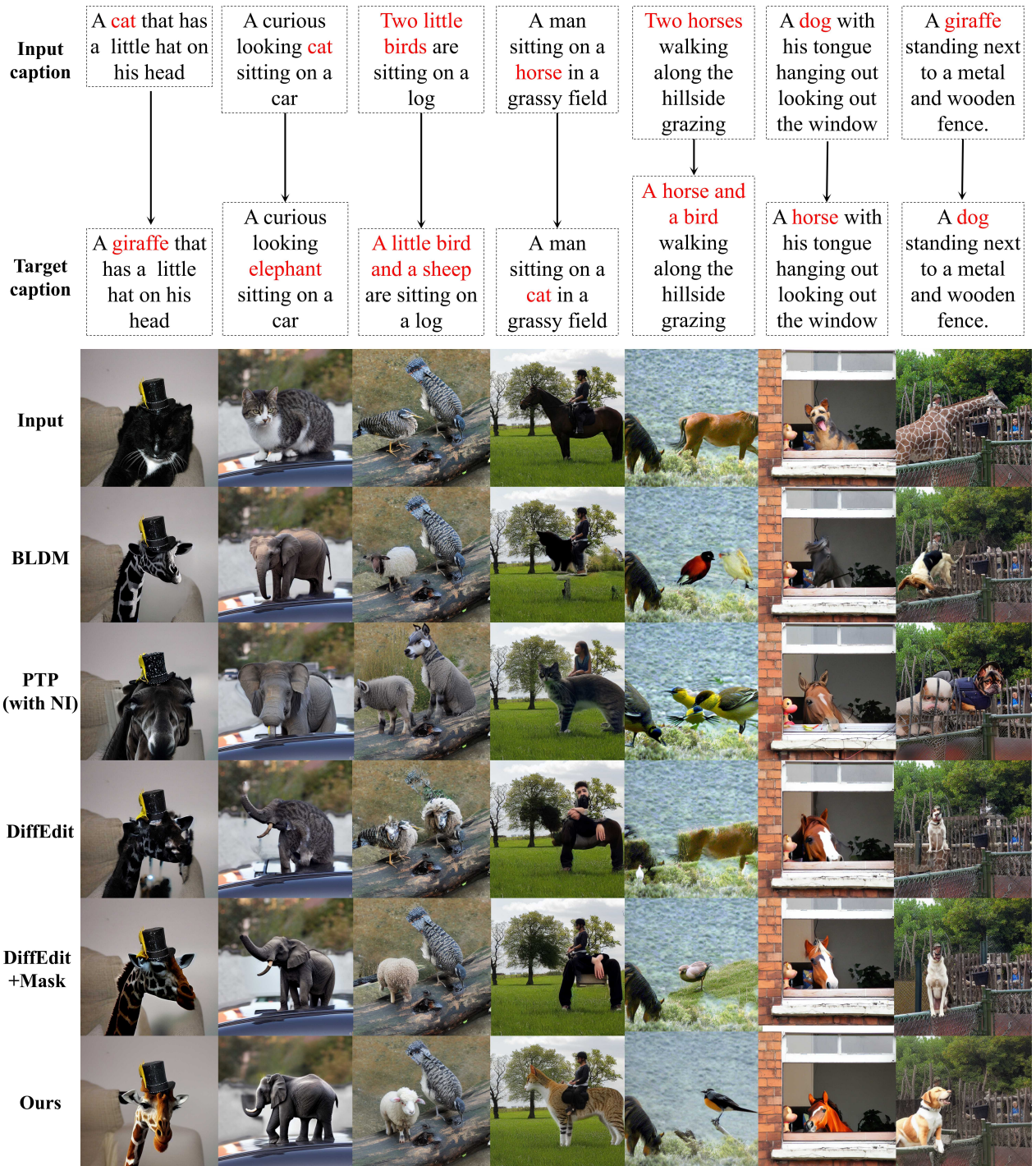


Figure 14. Qualitative results of different methods on foreground object editing on COCO [24] images. The first row is the input image, and the second row visualizes the masks used in mask-based methods (BLDM [4], Ours).

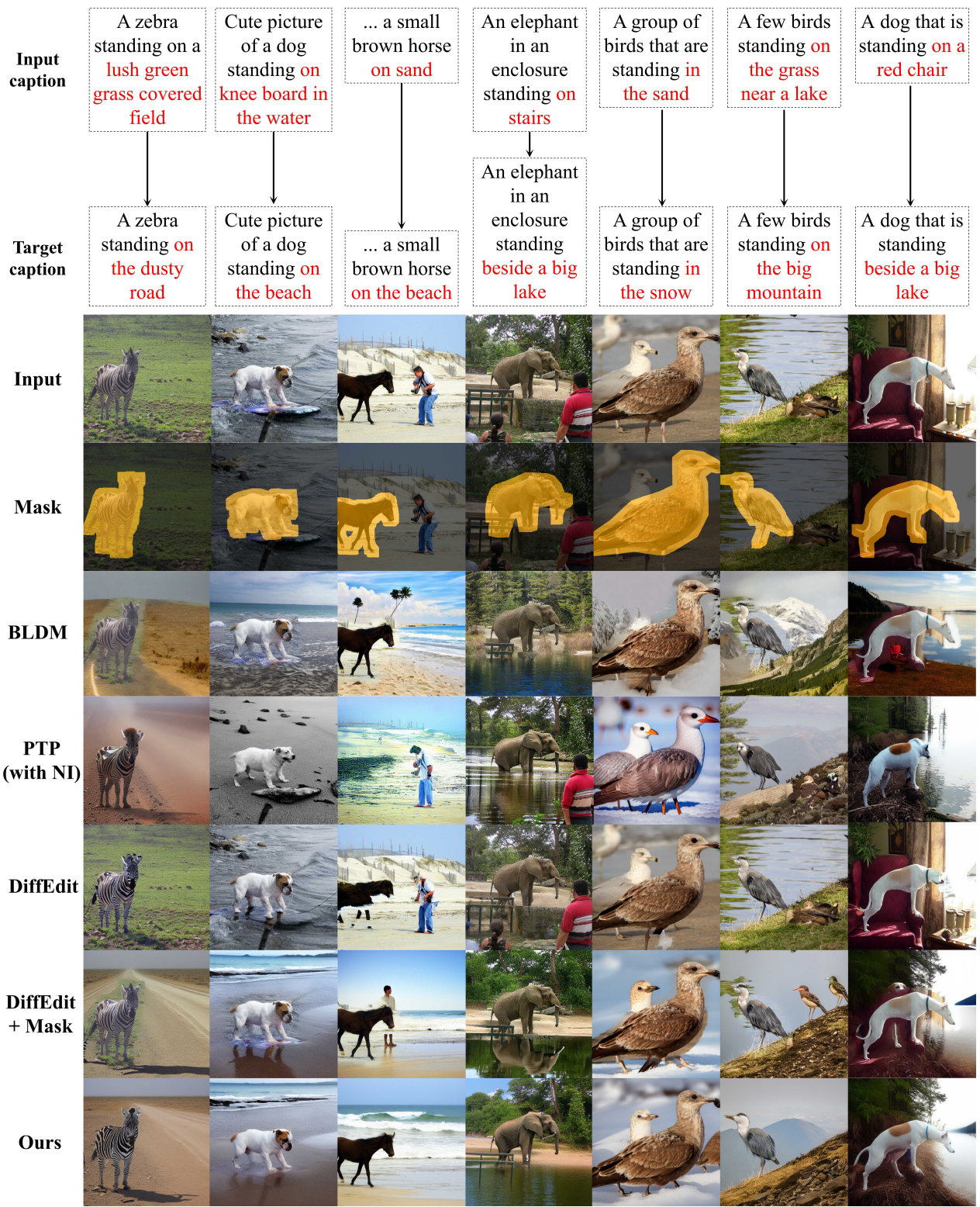


Figure 15. Qualitative results of different methods on background editing on COCO [24] images. The first row shows input images, and the second row visualizes the masks used in mask-based methods (BLDM [4], Ours).